Acta Scientiae Veterinariae, 2026. 54: 2016.

RESEARCH ARTICLE
Pub. 2016

ISSN 1679-9216

Porcine ARAF Interaction with MST2 Regulated Apoptosis in PK-15 Cells

Linwei Dai[1*], Kangzhi Xu[1*], Zhiyong Han[1], Jiexin Yin[2], Beibei Li[1], Jing Ma[1], Mingyue Zu[1], Jianping Tao[1] & Zhaofeng Hou[1]

ABSTRACT

***Background*:** Apoptosis is a conserved cellular process essential for tissue homeostasis and host defense regulation. ARAF and MST2 are key serine/threonine kinases that regulate cell survival and apoptosis. However, whether these proteins directly interact and how their association affects apoptotic signaling remain unclear. In human cells, ARAF–MST2 interaction regulates apoptosis independently of the canonical Raf/MEK/ERK pathway. Therefore, this study aimed to determine whether porcine ARAF interacts with MST2 and to elucidate the molecular mechanism by which this interaction influences apoptosis in PK-15 cells.

***Materials, Methods & Results*:** Coding sequences of porcine *ARAF* and *MST2* genes were amplified, cloned into pcDNA3.1 expression vectors with N-terminal Flag and HA epitope tags, verified by Sanger sequencing, and transiently transfected into PK-15 cells. Bioinformatic analyses using STRING and AlphaFold3 predicted a strong physical association between ARAF and MST2, with the predicted interaction interface involving several conserved residues within α-helical and random-coil domains. Structural visualization through PyMOL and secondary structure prediction by SOPMA and SWISS-MODEL revealed highly conserved domains consistent with functional interaction potential. Co-immunoprecipitation assays verified the formation of the ARAF–MST2 complex in PK-15 cells, and immunofluorescence microscopy demonstrated that both proteins predominantly co-localized in the cytoplasm, in agreement with UniProt-based localization predictions. Functional assays revealed that ARAF overexpression markedly reduced PK-15 cell apoptosis, as determined by Annexin V/PI flow cytometric analysis. Western blot and quantitative PCR analyses further showed that ARAF overexpression led to significant suppression of MST2 phosphorylation at threonine 180 (p-MST2 T180), accompanied by increased total MST2 and BCL-2 levels, and decreased pro-apoptotic BAX and cleaved caspase-3 (Cl-caspase3) expression. Conversely, when MST2 activation was enhanced, apoptotic signaling was restored, indicating that ARAF modulates cell fate through inhibition of MST2 activation. Statistical analyses, conducted via one-way ANOVA and t-tests across three biological replicates.

***Discussion*:** Collectively, these findings establish that porcine ARAF physically interacts with MST2 and exerts an anti-apoptotic effect by attenuating MST2 phosphorylation and activation. The discovery of the ARAF–MST2 axis as a negative regulator of apoptotic signaling expands our understanding of how Raf kinases integrate with Hippo pathway components to balance cellular survival and death. Given the evolutionary conservation of ARAF and MST2 across mammalian species, this study provides a new molecular framework for exploring how ARAF–MST2 crosstalk contributes to host–pathogen interactions, cellular stress responses, and the maintenance of homeostasis in porcine cells. Furthermore, the elucidation of this novel ARAF–MST2 signaling mechanism lays the groundwork for future research into its role in viral infections, oncogenic transformation, and other apoptosis-related diseases in swine and potentially in other mammals. Overall, our data indicate that the ARAF–MST2 complex functions as a pivotal modulator of cell fate by integrating pro- and anti-apoptotic cues within the cytoplasmic signaling network of PK-15 cells.

Keywords: ARAF, MST2, protein–protein interaction, apoptosis.

DOI: 10.22456/1679-9216.152983

Received: 10 January 2026 Accepted: 28 April 2026 Published: 11 May 2026

[*]Linwei Dai & Kangzhi Xu share first authorship. [1]College of Veterinary Medicine; Jiangsu Co-innovation Center for Prevention and Control of Important Animal Infectious Diseases and Zoonoses; Jiangsu Key Laboratory of Zoonosis, Yangzhou University (YZU); Yangzhou, China. [2]Jiangsu Agri-animal Husbandry Vocational College, Taizhou, China. CORRESPONDENCE: Zhaofeng Hou [zfhou@yzu.edu.cn]. College of Veterinary Medicine, Yangzhou University (YZU). 12 East Wenhui Road, Yangzhou, 225009 Jiangsu, China.

INTRODUCTION

ARAF (V-raf murine sarcoma 3611 viral oncogene homolog) belongs to the Raf serine/threonine kinase family, which includes ARAF, BRAF, and CRAF. Raf kinases regulate essential cellular processes such as differentiation, proliferation, metabolism, and apoptosis [16,37]. Their activation is triggered by Ras GTPases at the plasma membrane, leading to the sequential phosphorylation of MEK1/2 and ERK1/2 [20,41]. Notably, ARAF and CRAF can also influence cell cycle progression independently of downstream MEK/ERK signaling [10].

MST2 (mammalian STE20-like protein kinase 2), a serine/threonine kinase, plays essential roles in oxidative stress response, apoptosis, and proliferation [15,32]. MST kinases inhibit cell proliferation and promote apoptosis during embryogenesis [22,29]. MST1/2 has also been identified as a key component of the highly conserved Hippo signaling pathway in mammals [2,8,38]. This pathway primarily functions through a kinase cascade, with core components including MST1/2, LATS1/2, and YAP/TAZ [5], serving as important regulators of cell growth and development [38].

Our preliminary work demonstrated that MST2 activation in porcine PK-15 cells exerts a pro-apoptotic effect [35]. Previous studies have shown that ARAF and CRAF can suppress MST2 activation and MST2-induced apoptosis by binding to MST2 independently of their kinase activity [3,17,24,27,30]. Moreover, membrane relocalization of ARAF reduces its capacity to sequester MST2, thereby sensitizing cells to apoptosis [28]. However, the existence of a direct interaction between porcine ARAF and MST2, and its functional implications for apoptotic regulation, remain unclear.

MATERIALS AND METHODS

Protein-protein interaction (PPI) network analysis

To explore the potential interaction between porcine ARAF and MST2, PPI networks were constructed. The potential interacting proteins of ARAF and MST2 were predicted using the STRING database (version 12.0; https://string-db.org) [33], applying a medium confidence score cutoff of 0.4 and limiting the maximum number of interactors to 100. The obtained PPI network data were subsequently imported into Cytoscape software (version 3.10.3) [31] for visualization and topological analysis.

Amplification of the CDS regions of porcine ARAF and MST2 genes

Total RNA was extracted from PK-15 cells following the instructions of Fast Pure Cell/Tissue Total RNA Isolation Kit(#RC112)[1]. The concentration and purity of the extracted total RNA were measured using a Nanodrop spectrophotometer[7]. RNA with an OD260/280 ratio between 1.8 and 2.0 was used for reverse-transcribed into cDNA using a HiScript II 1st Strand cDNA Synthesis Kit (+gDNA wiper) [#R212][1] according to the manufacturer's protocol. Subsequently, specific primers were designed based on the CDS regions of porcine ARAF (XM_005657798.3)and MST2 (XM_005655350.3) from GenBank, aligning with restriction sites in the pcDNA3.1-3HA-C and pcDNA3.1-3Flag-C plasmids. For ARAF, primers F1 and R1 were designed with *EcoR I* and *Xho I* sites and protective bases, excluding the stop codon. For MST2, primers F2 and R2, containing homologous arms, were designed after stop codon removal. Additionally, primers F3 and R3 were designed for linearizing pcDNA3.1-3HA-C via inverse PCR. Primer sequences are provided in Table 1.

Construction and overexpression of recombinant eukaryotic expression plasmids for porcine ARAF and MST2

The *ARAF* gene product, containing restriction sites and protective bases, was gel-purified and double-digested with *EcoR I* (#1040)[2] and *Xho I* (#1040)2 alongside the pcDNA3.1-3Flag-C plasmid. And the gel-purified *MST2* gene product, containing homologous arms, was recombined with the linearized pcDNA3.1-3HA-C vector via ClonExpress II One Step Cloning Kit (#C112)[1] and transformed into DH5α cells (#9057)[2]. The digested fragments were ligated using T4 DNA ligase(#2011A)[2] and transformed into DH5α competent cells. Transformed cells were plated on ampicillin-resistant LB agar plates. Single colonies were selected, cultured, and subjected to plasmid extraction. The extracted plasmids were verified by double digestion, and positive clones were sequenced by BGI Genomics Co. Ltd[3]. The recombinant plasmidswere purified using an EndoFree Mini Plasmid Kit (#DP123)[4] according to the manufacturer's instructions. The constructs, designated as pcDNA3.1-3Flag-C-ARAF and pcDNA3.1-3HA-C-MST2, were transfected into PK-15 cells using Lipofectamine™ 3000 (#L3000015)[5].

Table 1. Primer Sequences used in the experiments.

Target gene	Primer sequence (5'→3')	Product length / bp	Annealing temperature (°C)	Purposes
ARAF	F1: CCGGAATTCATGGAGCCACCACGGGGC R1: CCGCTCGAGAGGCACAAGGCGGGCT	1836	60	Plasmid construction
MST2	F2: agtccagtgtggtggaattcATGGAGCAGCCGCCGGCG R2:acgtcgtatgggtactcgagAAAGTTCTGCTGCCTTCTTTTCTT	1513	62	Plasmid construction
pcDNA3.1-3HA-C	F3: CTCGAGTACCCATACGACGTACC R3: GAATTCCACCACACTGGACTAGTG	5485	59	Linearization of vector
ARAF	qF1: GGCAGTGGGCACCGTCAAAG qR1: CCTGATTGAGACCTCGCACCTTG	122	60	qPCR
MST2	qF2: TGGCTGACATCTCGTCCCTTGG qR2: TCCTGAATGTTGGTGGTGGGTTTG	126	60	qPCR
BAX	qF3: GGAGATGAACTGGACAGTAAC qR3: GCCGTCAGCAAACATTTC	111	60	qPCR
BCL-2	qF4: GCACCTGACTCCCTTCA qR4: ACTCAAAGAAGGCCACAATC	101	60	qPCR
GAPDH	qF3: GTCGGTTGTGGATCTGACCT qR3: CTTGACGAAGTGGTCGTTGA	208	60	qPCR

Note: The ARAF sequence is marked with underlined *EcoR I* and *Xho I* cleavage sites.

Bioinformatics analysis of porcine ARAF and MST2

The bioinformatics online tools SOPMA (https://npsa-pbil.ibcp.fr/cgi-bin/npsa_automat.pl?page=/NPSA/npsa_sopma.html), and SWISS-MODEL (https://swissmodel.expasy.org/) were utilized to analyze the secondary structures and tertiary structures of the proteins encoded by the porcine *ARAF* and *MST2* genes, respectively. The SMART online tool (http://smart.embl-heidelberg.de/) was employed to predict the structural domains of the porcine ARAF and MST2 protein. Subcellular localization predictions for the porcine ARAF and MST2 proteins were performed using the UniProt online tool (https://www.uniprot.org/). The AlphaFold[3] online tool (https://golgi.sandbox.google.com/about) was used to predict the interaction sites between porcine ARAF and MST2, and the PyMOL software was used to visualize the amino acid residues at the interaction sites of ARAF and MST2. Protein sequences of ARAF and MST2 from different species were downloaded from GenBank, and amino acid homology analysis was conducted using MegAlign software. The ESPript 3.2 (http://espript.ibcp.fr/ESPript/cgi-bin/ESPript.cgi) online tool was used to align the amino acid sequences of ARAF and MST2 across different species.

Quantitative real-time PCR (qPCR)

Total RNA samples were isolated from cells using FastPure Cell/Tissue Total RNA Isolation Kit, and 1 μg of total RNA was reverse transcribed into cDNAs using HiScript III All-in-one RT SuperMix Perfect for qPCR (#R333)[1]. Quantitative real-time PCR (qPCR) reactions were performed using the AceQ Universal SYBR qPCR Master Mix (#Q511)1 with triplicate of each. The relative expression levels of *ARAF, MST2, BAX, BCL-2* genes (primer sequences in Table 1) were quantified and normalized to glyceraldehyde-3-phosphate dehydrogenase (*GAPDH*) gene using the $2^{-\Delta\Delta Ct}$ method [13].

Western blot (WB)

Total proteins were extracted from cells using RIPA Lysis Buffer (#WB3100)[6]supplemented with protease and phosphatase inhibitor cocktail (#P002)[6]. Equal amounts of protein (50 μg) were separated by sodium dodecyl sulfate–polyacrylamide gel electrophoresis (SDS–PAGE) and subsequently transferred onto polyvinylidene fluoride (PVDF) membranes. The membranes were blocked with 3% non-fat milk at room temperature for 2 h, followed by incubation with primary antibodies overnight at 4°C. After washing five times with TBST, the membranes were incubated with horseradish peroxidase (HRP)-conjugated goat anti-rabbit IgG (#AS014)[7]or HRP-conjugated goat anti-mouse IgG (#AS003)[7] for 1 h at room temperature and then washed again five times with TBST. Protein bands were visualized using an enhanced chemiluminescence reaction buffer and imaged on a Tanon automatic chemiluminescence image analysis system[8]. Rabbit antibodies including anti-ARAF (#ab200653)[9], anti -MST2 (#A9036)[7], anti-phospho-MST2-T180 (#AP1094)[7], anti-Flag (#AE092)[7], anti-BAX (#A19684)[7], anti-BCL-2 (#A19693)[7] andanti-Cl-caspase[3] (#9661)[10]at a 1:1 000 dilution; Mouse antibodies, including anti-HA (#26D11)[11] and anti-GAPDH (#AC002)[11], were used as primary antibodies at a 1:5000 dilution to detect the respective target proteins.

Co-Immunoprecipitation (CO-IP)

After 24 h of co-transfection with recombinant eukaryotic expression plasmids, PK-15 cells were washed 3 times with PBS. Cells were lysed using Non-Denaturing Lysis Buffer (containing Proteinase Inhibitor Cocktail) according to the Universal IP/Co-IP Toolkit (#KTI1020)[12] protocol. The lysate was centrifuged at 13,400× *g* for 10 min at 4°C, and the supernatant was collected. Protein concentration was measured using the BCA method and adjusted for uniformity. Protein A/G Magnetic Beads (20 μL) were washed 3 times with 1× Wash Buffer, incubated with 2 μg of antibody for 30 min at room temperature on a vertical rotating mixer, and washed again. Subsequently, 1 mg of protein sample was added to the antibody-coated beads and incubated for 1 h. After washing, 50 μL of 1× SDS-PAGE loading buffer was added and heated at 100°C for 5 min.The samples were briefly centrifuged and placed on a magnetic rack, and the supernatant was collected for Western blot analysis.

Immunofluorescence assay (IFA)

After 24 h of transfection or co-transfection of PK-15 cells with the recombinant eukaryotic expression plasmids, the original medium was discarded, and 1 mL of 4% paraformaldehyde was added to fix the cells at room temperature for 15 min. The fixative was then removed, and 1 mL of 0.5% Triton X-100 was added to permeabilize the cells for 15 min. Subsequently, 1 mL of 3% skim milk was added to each well to block non-specific reactions at room temperature for 1 h. The cells were incubated overnight at 4°C with 1 mL of rabbit-derived Flag antibody and mouse-derived HA antibody as primary antibodies. Afterward, the cells were incubated at room temperature for 90 min with FITC-labeled goat anti-rabbit IgG (H+L) [#A0562][13] and CY3-labeled goat anti-mouse IgG (H+L) [#A0521][13] as secondary antibodies. Following secondary antibody incubation, commercially available DAPI was added to the 6-well plate. Each step was followed by 3 washes with PBS. Finally, an anti-fade mounting medium was applied, and the cell slides were inverted onto glass slides, with the edges sealed using nail polish. The slides were then observed under a laser confocal microscope.

Flow cytometry (FCM)

The apoptotic levels of PK-15 cells were determined following the instruction of Annexin V-FITC/PI Apoptosis Detection Kit (#C1062M)[13]. Briefly, cells were harvested and resuspended in 200 μL binding buffer, and were incubated with FITC-conjugated annexin V and propidium iodide at 4°C for 15 min in the dark. The apoptosis rates were analyzed using a CytoFLEX Flow Cytometer[14].

Statistical analysis

In this study, statistical data were representative of ≥ 3 independent experiments and presented as the mean ± standard deviation (SD). Comparisons between 2 groups were analyzed using the *t*-test, while comparisons among multiple groups were analyzed using one-way analysis of variance (ANOVA). Differences were considered statistically significant at a *P* value of <0.05. All statistical analyses were carried out using GraphPad Prism 8.0 software[15].

RESULTS

Prediction of the interaction between porcine ARAF and MST2

To investigate the potential relationship between porcine ARAF and MST2, PPI networks were constructed using the STRING database (medium confidence = 0.4; maximum number of interactors = 100) and visualized with Cytoscape software. The predicted ARAF-interacting protein network revealed that MST2 (STK3) was among the potential interaction partners of ARAF (Figure 1A). Similarly, analysis of the MST2-interacting protein network also identified ARAF as one of its predicted binding proteins (Figure 1B). These results consistently indicated a potential interaction between porcine ARAF and MST2.

Construction and expression of pcDNA3.1-3Flag-C-ARAF recombinant plasmid in PK-15 cells and analysis of ARAF Gene

The porcine *ARAF* gene (1,836 bp), flanked by restriction sites and protective bases, was amplified by PCR (Figure 2A). The recombinant over expression plasmid pcDNA3.1-3Flag-C-ARAF was validated through *EcoR I* and *Xho I* restriction digestion (Figure 2B). DNA sequencing (Figures 2C), qPCR (Figures 2D), and Western blotting (Figures 2E) confirmed successful over expression of Flag-ARAF in PK-15 cells.

Protein domain analysis revealed that the porcine ARAF protein contains a Raf-like Ras domain (RBD) located between amino acids 19–91, as well as a Protein Kinase C Conserved Region 1 (C1) domain between amino acids 99–144. A low-complexity domain, indicated by a pink bar, was found between amino acids 243 and 270 (Figure 2F). Amino acid homology analysis of porcine ARAF proteins was performed with human, mice, sheep, and other animal species using MegAlign software. The results showed that the homology between swine and human, as well as other animals, for ARAF proteins ranged from 72.4% to 100%. The highest homology of porcine ARAF was with the African warthog (100%), and the lowest homology was with the Rana temporaria (72.4%) [Figure 2G].

ESPript online tool was used to compare the amino acid sequences of ARAF (Figure 2H) proteins across swine, humans, mice, sheep, and other animals. Red indicates conserved sequences across all species, yellow represents amino acid homology ≥70% between species. The comprehensive analysis showed that ARAF proteins were highly conserved in mammals, including humans, swine, mice, sheep, African warthogs, cows, dogs, and whales, with the lowest homology observed with the non-mammalian Rana temporaria.

Construction and expression of pcDNA3.1-3HA-C-MST2 recombinant plasmid in PK-15 Cells and analysis of MST2 gene

The porcine *MST2* gene (1,513 bp), flanked by homology arms, was successfully amplified by PCR (Figure 3A). The recombinant overexpression plasmid pcDNA3.1-3HA-C-MST2 was validated via restriction digestion with *EcoR I* and *Xho I*, yielding fragments consistent with expected sizes (Figure 3B). DNA sequencing (Figure 3C), qPCR (Figure 3D), and Western blotting (Figure 3E) confirmed the efficient overexpression of the HA-MST2 fusion protein in transfected PK-15 cells.

Porcine MST2 protein contains a serine/threonine protein kinase (S_TKc) structural domain (amino acids 27 to 278) [Figure 3F]. The amino acid sequences of MST2 shares 100%, 98.6%, 98.4%, and 98.2% identities with the counterparts in warthog, cattle, dog, and human, respectively (Fig 3G).

ESPript online tool was used to compare the amino acid sequences of MST2 (Figure 3H) proteins across swine, humans, mice, sheep, and other animals. The comprehensive analysis showed that MST2 proteins were highly conserved in mammals, with the lowest homology observed with the non-mammalian Rana temporaria.

Secondary and tertiary structure and interaction site prediction of porcine ARAF and MST2 proteins

The secondary and tertiary structures of porcine ARAF and MST2 proteins, along with their interaction sites, were predicted using bioinformatics tools including SOPMA, SWISS-MODEL, and AlphaFold3. The results demonstrated distinct structural compositions: porcine ARAF exhibited 52.97% random coils, 26.57% α-helices, 14.85% extended strands, and 5.61% β-turns (Figure 4A), while porcine MST2 comprised 41.96% random coils, 43.38% α-helices, 10.18% extended strands, and 4.48% β-turns (Figure 4B). Tertiary structure predictions (Figure 4C & D) aligned with these secondary structure profiles, revealing that both

proteins are predominantly organized into random coils and α-helices.

Subcellular localization of porcine ARAF and MST2 proteins was predicted using the UniProt online tool. The results indicated that porcine ARAF is predominantly localized to the cytoplasm, while MST2 is predicted to localize to the cytoplasm, centrosome, and nucleus. These findings suggest potential co-localization and functional interplay between ARAF and MST2 within the cytoplasmic compartment.

AlphaFold3-based modeling further identified potential interaction regions between ARAF and MST2. The predicted template modeling (pTM) score and interface prediction template modeling (ipTM) score were 0.35 and 0.44, respectively. The predicted alignment error (PAE) matrix showed error values ranging from 1 to 1096 (Figure 4E). The predicted results indicated that the following residues interact between ARAF and MST2 proteins: ARAF protein at position 512 (Ile) and MST2 protein at position 178 (Arg), ARAF protein at position 515 (Arg) and MST2 protein at position 180 (Thr), ARAF protein at position 469 (Ser) and MST2 protein at position 179 (Asn), ARAF protein at position 515 (Arg) and MST2 protein at position 178 (Arg), and ARAF protein at position 585 (Ser) and MST2 protein at position 484 (Lys) [Figure 4F].

Validation of ARAF and MST2 interaction

To verify whether porcine ARAF and MST2 proteins interact within cells, recombinant eukaryotic expression plasmids pcDNA3.1-3Flag-C-ARAF and pcDNA3.1-3HA-C-MST2 were co-transfected into PK-15 cells. After 24 h of transfection, the cell lysate supernatant was collected for CO-IP experiments. Western blot results showed that the recombinant protein Flag-ARAF interacted with HA -MST2 (Figure 5A).

Additionally, Immunofluorescence results showed that after individual transfection of recombinant eukaryotic expression plasmids pcDNA3.1-3Flag-C-ARAF and pcDNA3.1-3HA-C-MST2 into PK-15 cells, both porcine ARAF and MST2 proteins were expressed in the cytoplasm, which was consistent with the predicted results. When the recombinant plasmids pcDNA3.1-3Flag-C-ARAF and pcDNA3.1-3HA-C-MST2 were co-transfected into PK-15 cells, the recombinant proteins Flag-ARAF and HA-MST2 co-localized in the cytoplasm (Figure 5B), indicating that porcine ARAF and MST2 proteins exhibit co-localization.

Overexpression of ARAF suppresses MST2 phosphorylation and apoptosis

To investigate the role of ARAF in the regulation of apoptosis, porcine PK-15 cells were transfected with Flag-tagged ARAF expression plasmids, and apoptosis was evaluated at 24 h and 36 h post-transfection. As shown by flow cytometry (Figure 6A), ARAF overexpression significantly reduced the proportion of apoptotic cells compared with the Flag control group. Quantitative analysis further confirmed a marked decrease in apoptosis rates at both 24 h and 36 h (Figure 6B). Western blot analysis revealed that ARAF overexpression markedly reduced the phosphorylation level of MST2 (p-MST2 T180), while increasing the total MST2 and BCL-2 protein levels and decreasing the expression of BAX and Cl-caspase3 (Figure 6C & D). These results suggest that ARAF negatively regulates MST2 activation and its downstream apoptotic signaling. Consistent with the protein expression patterns, qPCR analysis showed that ARAF overexpression significantly reduced BAX but increased MST2 and BCL-2 mRNA levels (Figure 6E). Collectively, these findings indicate that ARAF inhibits MST2 phosphorylation and suppresses apoptosis in PK-15 cells by modulating the balance between pro-apoptotic and anti-apoptotic factors.

DISCUSSION

Since the 1st *Raf* gene was identified in 1983, isolated from a murine sarcoma virus-transduced retrovirus oncogene [26], ARAF has clearly been the "ugly duckling" among the 3 mammalian Raf kinases, with most research over the past few decades focusing on CRAF and BRAF [4,7]. Among the Raf protein family members, ARAF has the lowest kinase activity toward the MEK protein. In cell lysates, BRAF binds and phosphorylates MEK1/2 much more efficiently than ARAF and CRAF. BRAF, as the oldest family member, has the strongest MEK activity, while ARAF and CRAF primarily function to regulate the level and duration of ERK activity [9,14,19,25]. It has been reported that the RAF kinase family is involved in the progression of tumors, especially BRAF and CRAF, whose mutations lead to various outcomes such as tumor metastasis and apoptosis [11]. However, mutations in ARAF have rarely been reported, and despite its many similarities to other subtypes, its biological function remains a mystery.

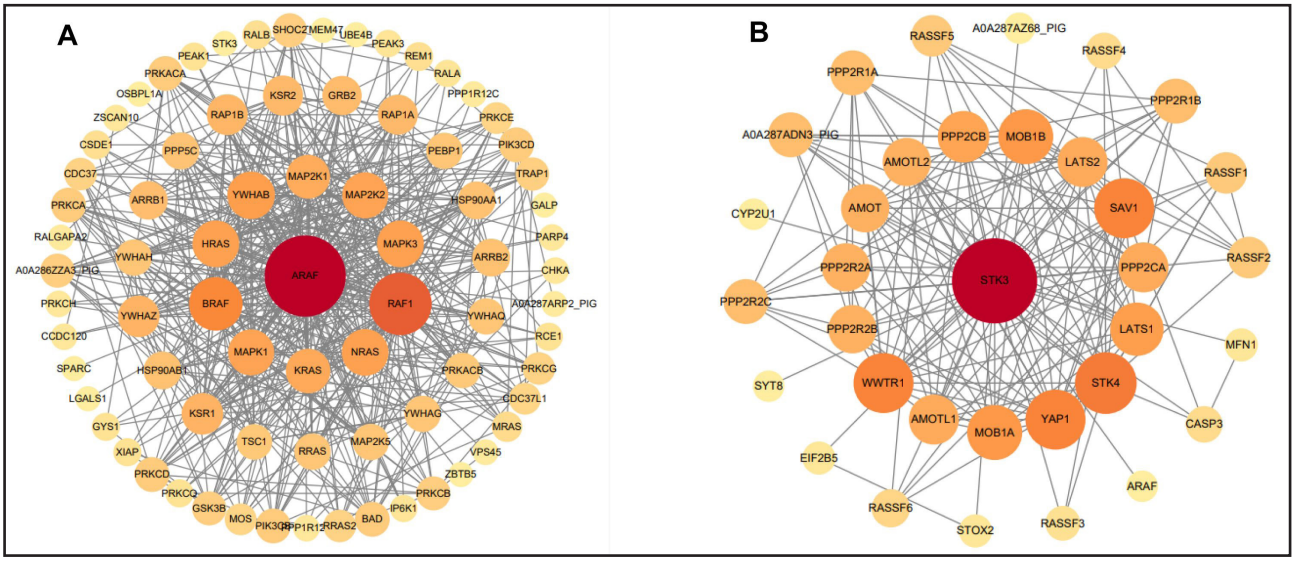

Figure 1. Predicted protein–protein interaction (PPI) networks of porcine ARAF and MST2 (STK3). A- PPI networks of the potential ARAF-interacting proteins were predicted using the STRING database (medium confidence=0.4; max number of interactors to show=100) and visualized with Cytoscape 3.10.3 software. B- PPI networks of the potential STK3-interacting proteins were predicted using the STRING database (medium confidence=0.4; max number of interactors to show=100) and visualized with Cytoscape 3.10.3 software.

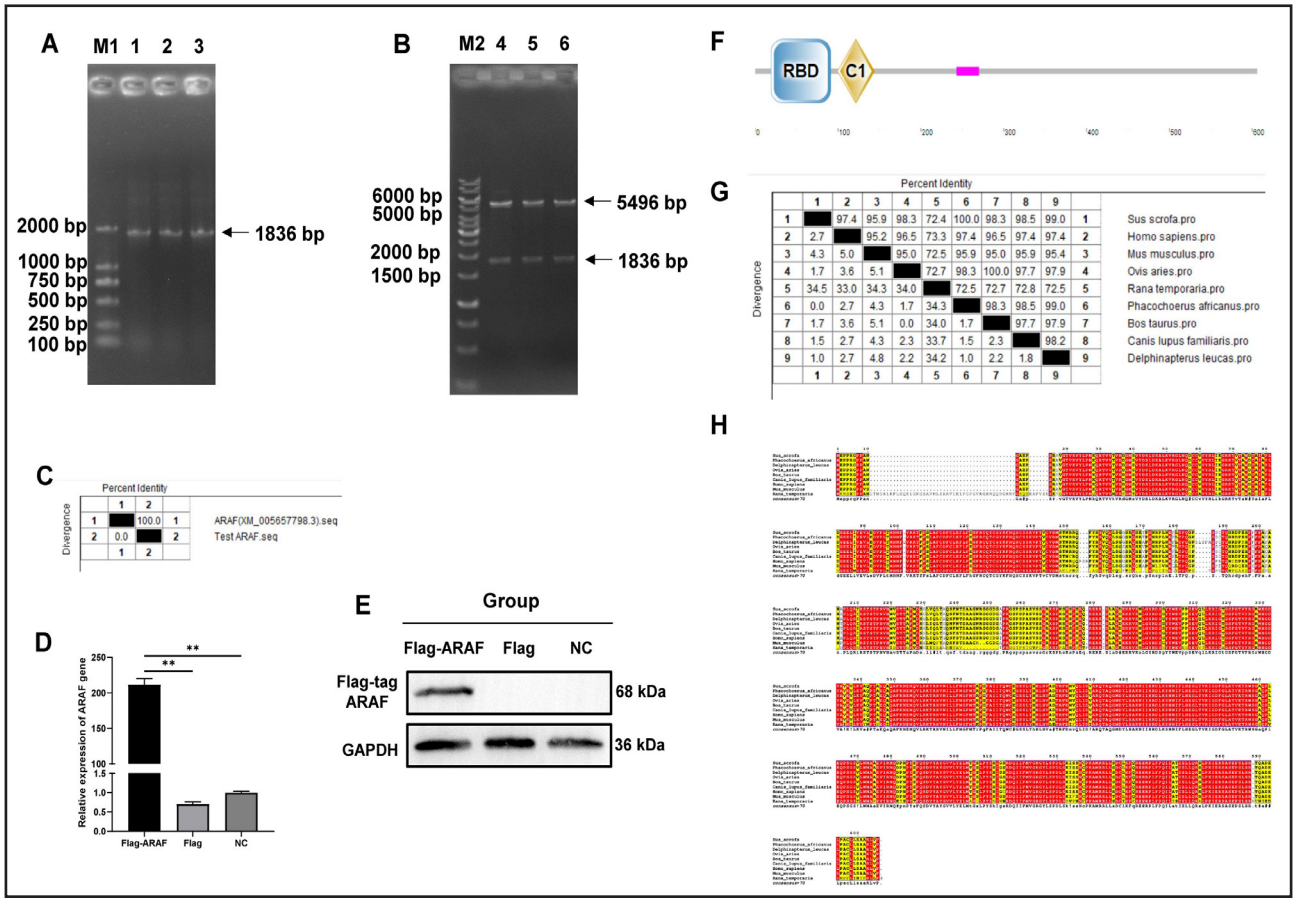

Figure 2. Expression of Flag-ARAF fusion protein and sequence analysis of the *ARAF* gene. A- RT-PCR amplification of the *ARAF* gene; M1: DL2000 DNA marker; 1,2,3: Results of the *ARAF* gene amplification. B- Restriction enzyme digestion with *EcoR I* and *Xho I* confirming successful plasmid construction; M2: 1kb DNA ladder; 4,5,6: Double digestion was performed on the pcDNA3.1-3Flag-C-ARAF plasmid. C- DNA sequencing demonstrating no base mutations in the *ARAF* gene. D- qPCR & E- Western blot analyses verifying successful overexpression of the *MST2* gene. F- Prediction of ARAF protein structural domains using the SMART program. G- Sequence distance analysis of ARAF from different species. The analysis was performed with MegAlign software. H- Use ESPript online tool to compare the ARAF amino acid sequences of pigs, humans, mice, sheep, and other animals. [All data are presented as the mean ± SD from at least 3 independent biological replicates. $^{**}P < 0.01$].

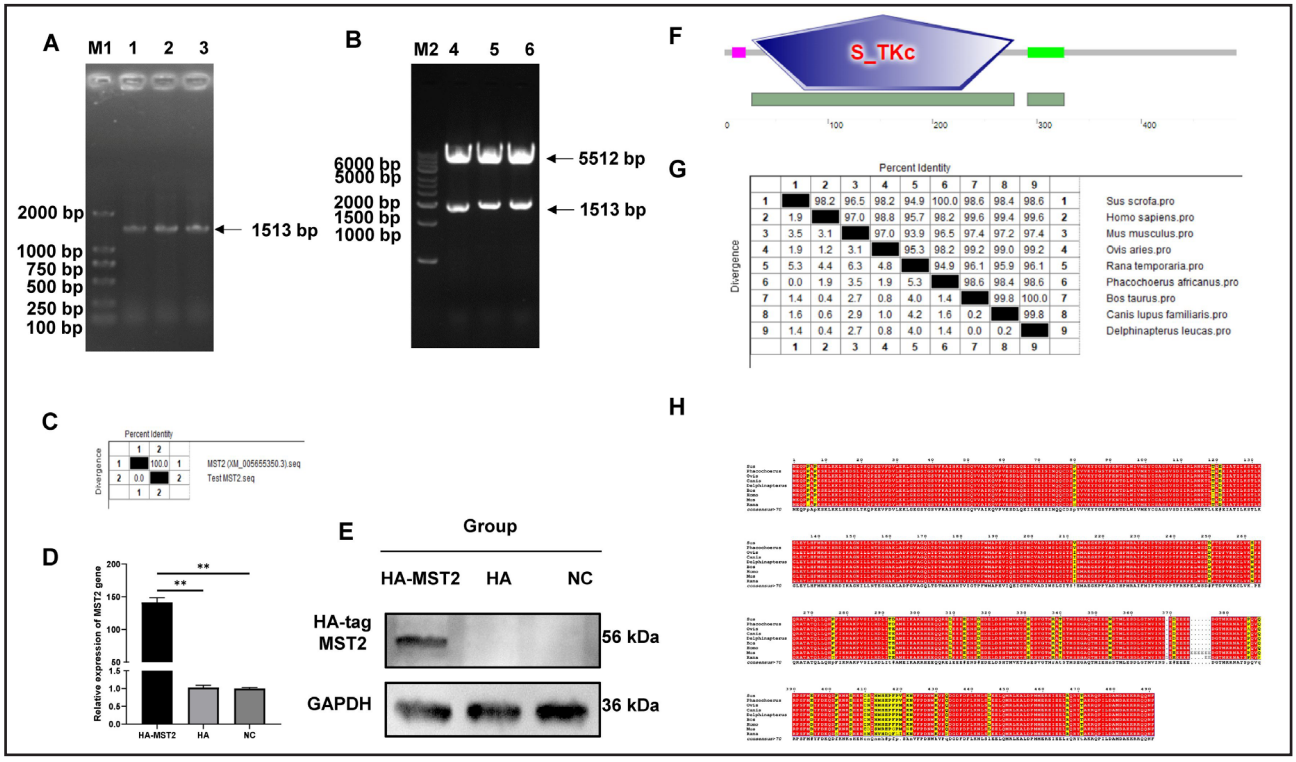

Figure 3. Expression of HA-MST2 fusion protein and sequence analysis of the *MST2* gene. A- RT-PCR amplification of the *MST2* gene; M1: DL2000 DNA marker; 1,2,3: Results of the *MST2* gene amplification. B- Restriction enzyme digestion with *EcoR I* and *Xho I* confirming successful plasmid construction; M2: 1kb DNA ladder; 4,5,6: Double digestion was performed on the pcDNA3.1-3Flag-C-MST2 plasmid. C- DNA sequencing demonstrating no base mutations in the *MST2* gene. D- qPCR & E- Western blot analyses verifying successful overexpression of the *MST2* gene. F- Prediction of *MST2* protein structural domains using the SMART program. G- Sequence distance analysis of MST2 from different species. The analysis was performed with MegAlign software. H- Use ESPript online tool to compare the MST2 amino acid sequences of pigs, humans, mice, sheep, and other animals. [All data are presented as the mean ± SD from at least three independent biological replicates. $^{**}P < 0.01$].

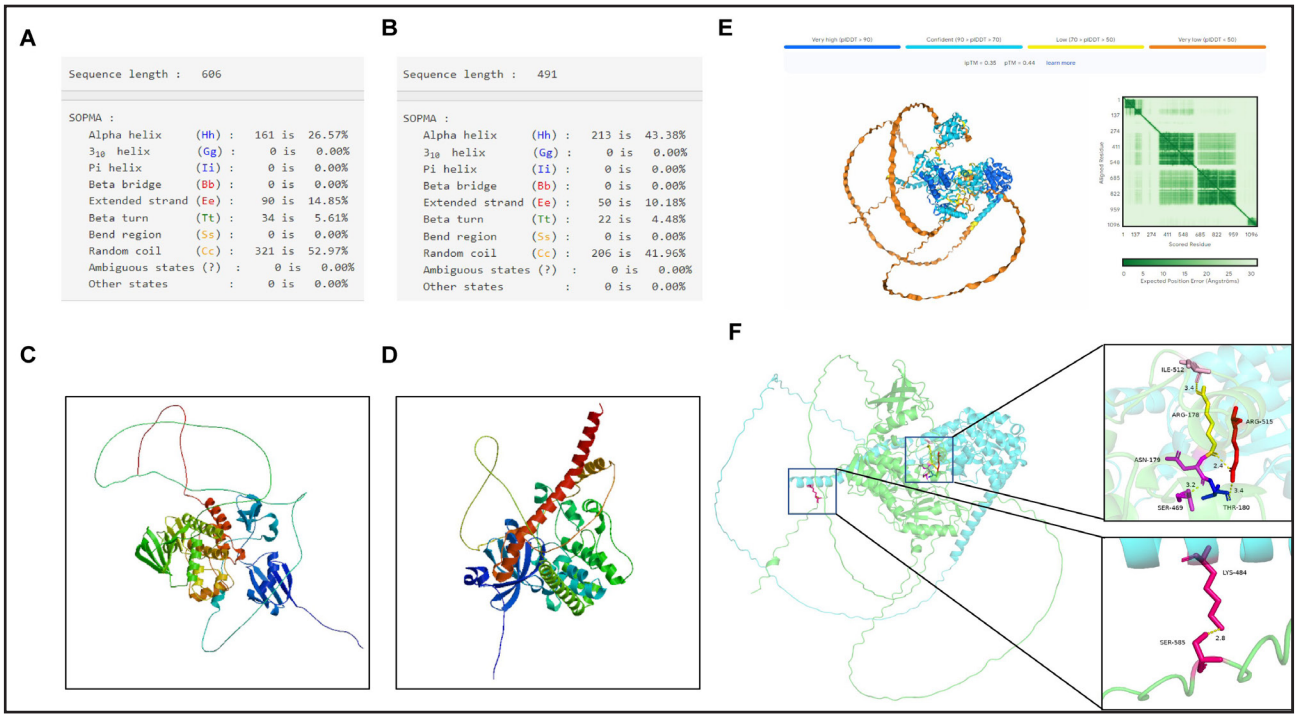

Figure 4. Secondary and Tertiary structure and interaction site prediction between ARAF and MST2 proteins. A- Predicted secondary structure of the ARAF protein using SOPMA. B- Predicted secondary structure of the MST2 protein using SOPMA. C- Predicted tertiary structure of the ARAF protein using SWISS-MODEL. D- Predicted tertiary structure of the MST2 protein using SWISS-MODEL. E- Interaction score prediction between ARAF and MST2 proteins using AlphaFold3. F- PyMOL visualization of the interaction sites between ARAF and MST2 proteins.

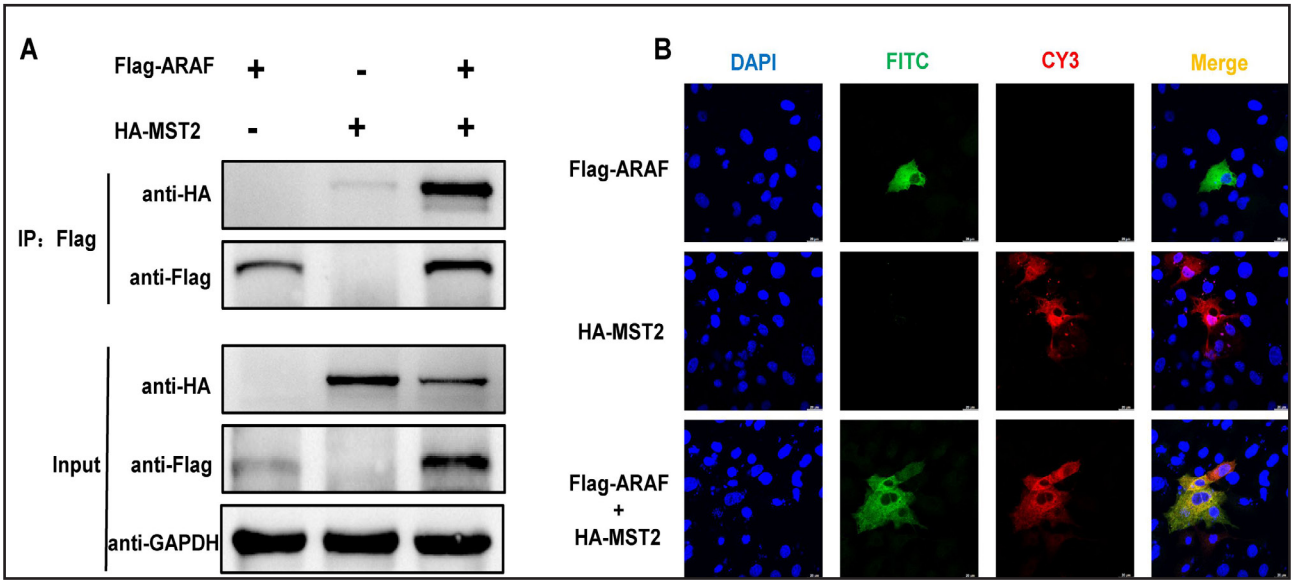

Figure 5. Interaction between porcine ARAF and MST2 proteins. A- Co-IP validation of the physical interaction between porcine ARAF and MST2 proteins. B- Co-localization of porcine ARAF and MST2 proteins in PK-15 cells. [Scale bars represent 20 μm].

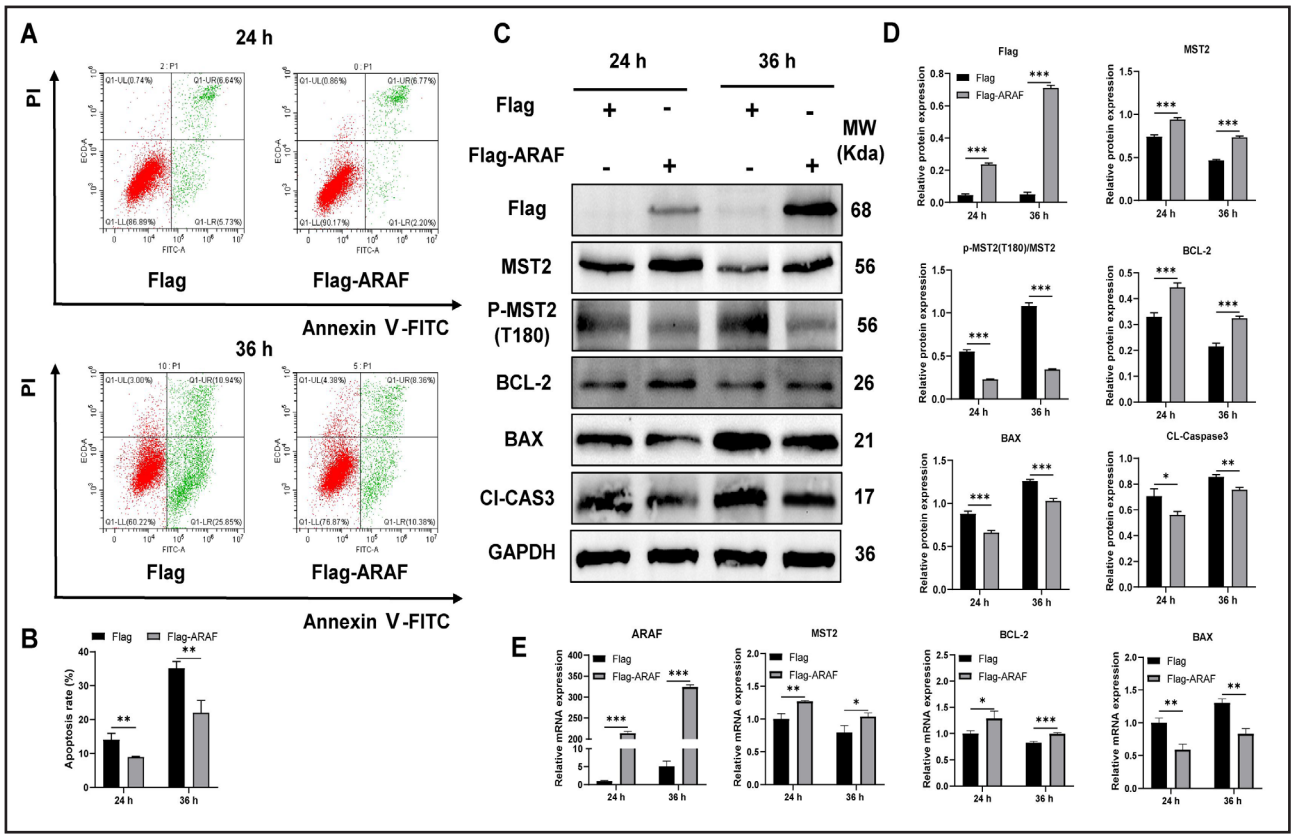

Figure 6. Porcine ARAF inhibits apoptosis by suppressing MST2 phosphorylation. A- Effects of ARAF overexpression on apoptosis in PK-15 cells at 24 h and 36 h after transfection with the pcDNA3.1-3×Flag-C-ARAF plasmid. B- Statistical analysis of apoptosis rates determined by flow cytometry. C- Effects of ARAF overexpression on MST2 phosphorylation and apoptosis-related proteins. D- Quantification of grayscale intensity of protein bands. E- Effects of ARAF overexpression on the mRNA expression levels of MST2, BAX, and BCL-2 as determined by qPCR. [All data are presented as mean ± SD from at least 3 biological replicates. ***$P < 0.001$; **$P < 0.01$; *$P < 0.05$].

MST1/2, as key signaling kinases in the Hippo signaling pathway, can be activated by autophosphorylation under oxidative stress. Activated MST1/2 can inhibit the expression of a series of anti-apoptotic factors through a kinase cascade reaction [1,42]. Conversely, activated anti-apoptotic factors such as BCL-2 can effectively suppress MST2-mediated apoptosis [34]. Cardiac-specific over-expression of Mst1 in mouse results in activation of caspases, increased apoptosis and dilated cardiomyopathy, whereas the inhibition of endogenous Mst1 prevents apoptosis of cardiomyocytes and cardiac dysfunction [21,36]. Overexpression of MST2 in lens cells has been shown to significantly increase cell apoptosis [12,35]. Moreover, gene knockout experiments have shown that knocking down MST1/2 can reduce the expression of p53 and the activity of Caspase-3, thereby inhibiting apoptosis [39,40]. These studies suggest that MST2, as one of the key members of the Hippo signaling pathway, plays a crucial role in regulating the outcomes of cell apoptosis through changes in its expression or phosphorylation activation.

Due to the low kinase activity of ARAF toward MEK, its physiological functions beyond the classical Raf/MEK/ERK pathway have gradually become a focus of research. During tumorigenesis, ARAF can function independently of its downstream MEK-ERK pathway by interacting with other proteins. It has been reported that ARAF and Raf-1 can strongly interact with MST2 in a kinase activity-independent manner, inhibiting MST2 phosphorylation and blocking its mediated Hippo signaling pathway, thereby suppressing apoptosis [23,27]. Additionally, ARAF and MST2 proteins have been shown to co-localize on mitochondria in tumor cell lines or primary tumors [28]. This inverse regulation of ARAF and MST2 signaling suggests that, during evolution, the role of RAF has shifted from exclusively activating the ERK pathway to regulating other cellular processes. Furthermore, ARAF interacts with PKM2, which is highly expressed in cancer cells. ARAF-mediated transformation can convert PKM2 from a low-activity dimer to a high-activity tetramer, thereby enhancing PKM2 activity [6,18]. These findings indicate that ARAF exerts diverse biological functions in cellular regulation. Our study demonstrates that porcine ARAF interacts with MST2 and negatively regulates apoptosis by inhibiting MST2 phosphorylation. This conclusion is supported by the observation that ARAF overexpression increases the expression of total MST2 and the anti-apoptotic protein BCL-2, while decreasing the levels of phosphorylated MST2 (p-MST2-T180), BAX, and Cl-caspase3 in a time-dependent manner.

In summary, this study confirmed the interaction between porcine ARAF and MST2, which co-localize in the cytoplasm and are highly conserved among mammals. These results provide a theoretical basis for exploring the regulatory mechanisms of ARAF–MST2 signaling in apoptosis and its potential involvement in porcine disease processes.

CONCLUSION

Our study identifies the porcine ARAF–MST2 complex as a critical regulator of apoptosis. Co-immunoprecipitation and immunofluorescence assays confirmed the direct interaction and cytoplasmic co-localization of ARAF and MST2. Mechanistic analyses revealed that ARAF inhibits MST2 phosphorylation, leading to reduced activation of pro-apoptotic proteins BAX and Cl-caspase3, while enhancing the expression of anti-apoptotic BCL-2. Structural predictions generated by AlphaFold3 further revealed conserved interaction interfaces primarily composed of α-helical and random coil domains. These findings establish the ARAF–MST2 axis as a novel modulatory pathway in porcine apoptosis regulation and provide a molecular basis for future investigations into its structural features and potential roles in host–pathogen interactions.

MANUFACTURERS

[1]Vazyme Biotech Co. Ltd. Nanjing, Jiangsu, China.

[2]TaKaRa Bio Inc. Shiga, Japan.

[3]BGI-Huada. Shenzhen, China.

[4]Tiangen Biotech Co. Ltd. Beijing, China.

[5]Thermo Fisher Scientific. Waltham, MA, USA.

[6]NCM, Suzhou Liankai Precise Mold Co. Ltd. Jiangsu, China.

[7]ABclonal Biotechnology Co. Ltd. Wuhan, Hubei, China.

[8]Tanon Science & Technology Co. Ltd. Shanghai, China.

[9]Abcam. Cambridge, MA, USA.

[10]Cell Signaling Technology. Danvers, MA, USA.

[11]Abmart Shanghai Co. Ltd. Shanghai, China.

[12]Abbkine Scientific Co. Ltd. Wuhan, China.

[13]Beyotime Biotech Inc. Shanghai, China.

[14]Beckman Coulter Inc. Shanghai, China.

[15]GraphPad Software. San Diego, CA, USA.

***Funding*.**This study was funded by the National Natural Science Foundation of China (No. 32373041 and 32002303 to Z.-F.H.), the National College Student Innovation and

Entrepreneurship Training Program (No. 202411117011Z to L.-W.D.), the Postgraduate Research & Practice Innovation Program of Jiangsu Province (No. SJCX23_2009 to K.-Z.X.), the China Postdoctoral Science Foundation (No. 2020M671615 to Z.-F.H.), the Basic Research Program of Jiangsu Province (No. BK20190885 to Z.-F.H.), the 111 Project (D18007) and a project funded by the Priority Academic Program Development of Jiangsu Higher Education Institutions (PAPD). The funders had no role in study design, data collection and analysis, decision to publish, or preparation of the manuscript.

***Acknowledgments*.** We especially thank the Testing Center of Yangzhou University for providing technical support.

***Declaration of interest*.** The authors report no conflicts of interest. The authors alone are responsible for the content and writing of the paper.

REFERENCES

1 **Ardestani A., Lupse B. & Maedler K. 2018.** Hippo Signaling: Key Emerging Pathway in Cellular and Whole-Body Metabolism. *Trends in Endocrinology and Metabolism: TEM*. 29(7): 492-509.DOI:10.1016/j.tem.2018.04.006.

2 **Avruch J., Zhou D., Fitamant J., Bardeesy N., Mou F. & Barrufet L.R. 2012.** Protein kinases of the Hippo pathway: regulation and substrates. *Seminars in Cell & Developmental Biology*. 23(7): 770-784. DOI: 10.1016/j.semcdb.2012.07.002.

3 **Beazely M.A., Alan J.K. & Watts V.J. 2005.** Protein kinase C and epidermal growth factor stimulation of Raf1 potentiates adenylyl cyclase type 6 activation in intact cells. *Molecular Pharmacology*. 67(1): 250-259. DOI:10.1124/mol.104.001370.

4 **Bonner T.I., Kerby S.B., Sutrave P., Gunnell M.A., Mark G. & Rapp U.R. 1985.** Structure and biological activity of human homologs of the raf/mil oncogene. *Molecular and Cellular Biology*. 5(6): 1400-1407. DOI:10.1128/mcb.5.6.1400-1407.1985.

5 **Cairns L., Tran T. & Kavran J.M. 2017.** Structural Insights into the Regulation of Hippo Signaling. *ACS Chemical Biology*. 12(3): 601-610. DOI:10.1021/acschembio.6b01058.

6 **Christofk H.R., Vander Heiden M.G., Harris M.H., Ramanathan A., Gerszten R.E., Wei R., Fleming M.D., Schreiber S.L. & Cantley L.C. 2008.** The M2 splice isoform of pyruvate kinase is important for cancer metabolism and tumour growth. *Nature*. 452(7184): 230-233. DOI:10.1038/nature06734.

7 **Davies H., Bignell G.R., Cox C., Stephens P., Edkins S., Clegg S., Teague J., Woffendin H., Garnett M.J., Bottomley W., Davis N., Dicks E., Ewing R., Floyd Y., Gray K., Hall S., Hawes R., Hughes J., Kosmidou V., Menzies A., Mould C., Parker A., Stevens C., Watt S., Hooper S., Wilson R., Jayatilake H., Gusterson B.A., Cooper C., Shipley J., Hargrave D., Pritchard-Jones K., Maitland N., Chenevix-Trench G., Riggins G.J., Bigner D.D., Palmieri G., Cossu A., Flanagan A., Nicholson A., Ho J.W.C., Leung S.Y., Yuen S.T., Weber B.L., Seigler H.F., Darrow T.L., Paterson H., Marais R., Marshall C.J., Wooster R., Stratton M.R. & Futreal P.A. 2002.** Mutations of the BRAF gene in human cancer. *Nature*. 417(6892): 949-954. DOI:10.1111/ced.12015.

8 **Du X., Dong Y., Shi H., Li J., Kong S., Shi D., Sun L.V., Xu T., Deng K. & Tao W. 2014.** Mst1 and mst2 are essential regulators of trophoblast differentiation and placenta morphogenesis. *PloS One*. 9(3): e90701. DOI: 10.1371/journal.pone.0090701.

9 **Han M., Golden A., Han Y. & Sternberg P.W. 1993.** C. elegans lin-45 raf gene participates in let-60 ras-stimulated vulval differentiation. *Nature*. 363(6425): 133-140. DOI:10.1038/363133a0.

10 **Karasarides M., Chiloeches A., Hayward R., Niculescu-Duvaz D., Scanlon I., Friedlos F., Ogilvie L., Hedley D., Martin J., Marshall C.J., Springer C.J. & Marais R. 2004.** B-RAF is a therapeutic target in melanoma. *Oncogene*. 23(37): 6292-6298. DOI:10.1038/sj.onc.1207785.

11 **Khan P.S., Rajesh P., Rajendra P., Chaskar M.G., Rohidas A. & Jaiprakash S. 2022.** Recent advances in B-RAF inhibitors as anticancer agents. *Bioorganic Chemistry*. 120: 105597. DOI:10.1016/j.bioorg.2022.105597.

12 **Liu S., Su D., Sun Z., Guan L., Wang Z., Zhang G., Zheng G., Cui T., Ma X. & Hu S. 2022.** High MST2 expression regulates lens epithelial cell apoptosis in age-related cataracts through YAP1 targeting GLUT1. *Archives of Biochemistry and Biophysics*. 723: 109255. DOI:10.1016/j.abb.2022.109255.

13 **Livak K.J. & Schmittgen T.D. 2001.** Analysis of relative gene expression data using real-time quantitative PCR and the 2(-Delta Delta C(T)) Method. *Methods*. 25(4): 402-408. DOI:10.1006/meth.2001.1262.

14 Marais R., Light Y., Paterson H.F., Mason C.S. & Marshall C.J. 1997. Differential regulation of Raf-1, A-Raf, and B-Raf by oncogenic ras and tyrosine kinases. *The Journal of Biological Chemistry*. 272(7): 4378-4383. DOI:10.1074/jbc.272.7.4378.

15 Masliantsev K., Karayan-Tapon L. & Guichet P.-O. 2021. Hippo Signaling Pathway in Gliomas. *Cells*. 10(1): 184. DOI:10.3390/cells10010184.

16 Matallanas D., Birtwistle M., Romano D., Zebisch A., Rauch J., von Kriegsheim A. & Kolch W. 2011. Raf family kinases: old dogs have learned new tricks. *Genes & Cancer*. 2(3): 232-260. DOI: 10.1177/1947601911407323.

17 Matallanas D., Romano D., Yee K., Meissl K., Kucerova L., Piazzolla D., Baccarini M., Vass J.K., Kolch W. & O'neill E. 2007. RASSF1A elicits apoptosis through an MST2 pathway directing proapoptotic transcription by the p73 tumor suppressor protein. *Molecular Cell*. 27(6): 962-975. DOI:10.1016/j.molcel.2007.08.008.

18 Mazurek S., Drexler H.C.A., Troppmair J., Eigenbrodt E. & Rapp U.R. 2007. Regulation of pyruvate kinase type M2 by A-Raf: a possible glycolytic stop or go mechanism. *Anticancer Research*. 27(6B): 3963-3971.PMID: 18225557.

19 McCubrey J.A., Steelman L.S., Hoyle P.E., Blalock W.L., Weinstein-Oppenheimer C., Franklin R.A., Cherwinski H., Bosch E. & McMahon M. 1998. Differential abilities of activated Raf oncoproteins to abrogate cytokine dependency, prevent apoptosis and induce autocrine growth factor synthesis in human hematopoietic cells. *Leukemia*. 12(12): 1903-1929. DOI:10.1038/sj.leu.2401215.

20 Moodie S.A., Willumsen B.M., Weber M.J. & Wolfman A. 1993. Complexes of Ras.GTP with Raf-1 and mitogen-activated protein kinase kinase. *Science*. 260(5114): 1658-1661. DOI:10.1126/science.8503013.

21 Odashima M., Usui S., Takagi H., Hong C., Liu J., Yokota M. & Sadoshima J. 2007. Inhibition of endogenous Mst1 prevents apoptosis and cardiac dysfunction without affecting cardiac hypertrophy after myocardial infarction. *Circulation Research*. 100(9): 1344-1352. DOI:10.1161/01.RES.0000265846.23485.7a.

22 Oh S., Lee D., Kim T., Kim T.-S., Oh H.J., Hwang C.Y., Kong Y.Y., Kwon K.S. & Lim D.S. 2009. Crucial role for Mst1 and Mst2 kinases in early embryonic development of the mouse. *Molecular and Cellular Biology*. 29(23): 6309-6320. DOI:10.1128/MCB.00551-09.

23 O'Neill E. & Kolch W. 2005. Taming the Hippo: Raf-1 controls apoptosis by suppressing MST2/Hippo. *Cell Cycle (Georgetown, Tex.)*. 4(3): 365-367. DOI:10.4161/cc.4.3.1531.

24 O'Neill E., Rushworth L., Baccarini M. & Kolch W. 2004. Role of the kinase MST2 in suppression of apoptosis by the proto-oncogene product Raf-1. *Science*. 306(5705): 2267-2270. DOI:10.1126/science.1103233.

25 Pritchard C.A., Samuels M.L., Bosch E. & McMahon M. 1995. Conditionally oncogenic forms of the A-Raf and B-Raf protein kinases display different biological and biochemical properties in NIH 3T3 cells. *Molecular and Cellular Biology*. 15(11): 6430-6442. DOI:10.1128/MCB.15.11.6430.

26 Rapp U.R., Goldsborough M.D., Mark G.E., Bonner T.I., Groffen J., Reynolds F.H. & Stephenson J.R. 1983. Structure and biological activity of v-raf, a unique oncogene transduced by a retrovirus. *Proceedings of the National Academy of Sciences of the United States of America*. 80(14): 4218-4222. DOI: 10.1073/pnas.80.14.4218.

27 Rauch J., O'Neill E., Mack B., Matthias C., Munz M., Kolch W. & Gires O. 2010. Heterogeneous nuclear ribonucleoprotein H blocks MST2-mediated apoptosis in cancer cells by regulating A-Raf transcription. *Cancer Research*. 70(4): 1679-1688. DOI: 10.1158/0008-5472.CAN-09-2740.

28 Rauch J., Vandamme D., Mack B., McCann B., Volinsky N., Blanco A., Gires O. & Kolch W. 2016. Differential localization of A-Raf regulates MST2-mediated apoptosis during epithelial differentiation. *Cell Death and Differentiation.* 23(8): 1283-1295. DOI:10.1038/cdd.2016.2.

29 Rawat S.J. & Chernoff J. 2015. Regulation of mammalian Ste20 (Mst) kinases. *Trends in Biochemical Sciences*. 40(3): 149-156. DOI:10.1016/j.tibs.2015.01.001.

30 Romano D., Nguyen L.K., Matallanas D., Halasz M., Doherty C., Kholodenko B.N. & Kolch W. 2014. Protein interaction switches coordinate Raf-1 and MST2/Hippo signalling. *Nature Cell Biology*. 16(7): 673-684. DOI:10.1038/ncb2986.

31 Shannon P., Markiel A., Ozier O., Baliga N.S., Wang J.T., Ramage D., Amin N., Schwikowski B. & Ideker T. 2003. Cytoscape: a software environment for integrated models of biomolecular interaction networks. *Genome Research*. 13(11): 2498-2504. DOI:10.1101/gr.1239303.

32 Sharma J., Antenos M. & Madan P. 2021. A Comparative Analysis of Hippo Signaling Pathway Components during Murine and Bovine Early Mammalian Embryogenesis. *Genes*. 12(2): 281. DOI:10.3390/genes12020281.

33 Szklarczyk D., Morris J.H., Cook H., Kuhn M., Wyder S., Simonovic M., Santos A., Doncheva N.T., Roth A., Bork P., Jensen L.J. & von Mering C. 2017. The STRING database in 2017: quality-controlled protein-protein association networks, made broadly accessible. *Nucleic Acids Research*. 45(D1): D362-D368. DOI:10.1093/nar/gkw937.

34 Won G.W., Park S.H., Park J., Lee Y. & Lee Y.H. 2019. Mammalian Hippo kinase pathway is downregulated by BCL-2 via protein degradation. *Biochemical and Biophysical Research Communications*. 512(1): 87-92. DOI:10.1016/j.bbrc.2019.03.015.

35 Xu K., Zhu S., Xu F., Yang J., Deng B., Su D., Ma J., Zu M., Lin Y., Pei T., Zhu Y., Wang L., Liu D., Duan Q., Xu J., Pan Z., Tao J. & Hou Z. 2024. Toxoplasma gondii induces MST2 phosphorylation mediating the activation of hippo signaling pathway to promote apoptosis and lung tissue damage. *iScience*. 27(12): 111312. DOI: 10.1016/j.isci.2024.111312.

36 Yamamoto S., Yang G., Zablocki D., Liu J., Hong C., Kim S.J., Soler S., Odashima M., Thaisz J., Yehia G., Molina C.A., Yatani A., Vatner D.E., Vatner S.F. & Sadoshima J. 2003. Activation of Mst1 causes dilated cardiomyopathy by stimulating apoptosis without compensatory ventricular myocyte hypertrophy. *The Journal of Clinical Investigation*. 111(10): 1463-1474. DOI:10.1172/JCI17459.

37 Yoon S. & Seger R. 2006. The extracellular signal-regulated kinase: multiple substrates regulate diverse cellular functions. *Growth Factors*. 24(1): 21-44. DOI:10.1080/02699050500284218.

38 Yu F.-X., Zhao B. & Guan K.-L. 2015. Hippo Pathway in Organ Size Control, Tissue Homeostasis, and Cancer. *Cell*. 163(4): 811-828. DOI:10.1016/j.cell.2015.10.044.

39 Zhang J., Liu J., Gao S., Lin W., Gao P., Gao K., Zhang Y., Du K., Yang X., Wang W., Zhu R. & Wang Y. 2019. Antiapoptosis and Antifibrosis Effects of Qishen Granules on Heart Failure Rats via Hippo Pathway. *BioMed Research International*. 2019: 1642575. DOI: 10.1155/2019/1642575.

40 Zhang Q., Cheng X., Zhang H., Zhang T., Wang Z., Zhang W. & Yu W. 2020. Dissecting molecular mechanisms underlying H2O2-induced apoptosis of mouse bone marrow mesenchymal stem cell: role of Mst1 inhibition. *Stem Cell Research & Therapy*. 11(1): 526. DOI:10.1186/s13287-020-02041-7.

41 Zhang X.F., Settleman J., Kyriakis J.M., Takeuchi-Suzuki E., Elledge S.J., Marshall M.S., Bruder J.T., Rapp U.R. & Avruch J. 1993. Normal and oncogenic p21ras proteins bind to the amino-terminal regulatory domain of c-Raf-1. *Nature*. 364(6435): 308-313. DOI:10.1038/364308a0.

42 Zheng Y. & Pan D. 2019. The Hippo Signaling Pathway in Development and Disease. *Developmental Cell*. 50(3): 264-282. DOI:10.1016/j.devcel.2019.06.003.